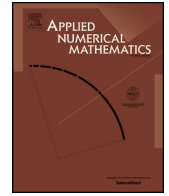


Contents lists available at [ScienceDirect](https://www.sciencedirect.com)

Applied Numerical Mathematics

www.elsevier.com/locate/apnum

Computing eigenvalues and eigenfunctions of the Laplacian for convex polygons



Matthew J. Colbrook^{a,*}, Athanasios S. Fokas^{a,b}

^a DAMTP, Centre for Mathematical Sciences, University of Cambridge, Wilberforce Rd, Cambridge CB3 0WA, United Kingdom

^b Viterbi School of Engineering, University of Southern California, Los Angeles, CA, 90089, USA

ARTICLE INFO

Article history:

Received 20 July 2017

Received in revised form 1 December 2017

Accepted 1 December 2017

Available online 6 December 2017

Keywords:

Elliptic PDEs

Eigenvalues and eigenfunctions

Boundary value problems

Spectral convergence

Unified transform method

ABSTRACT

Recently a new transform method, called the Unified Transform or the Fokas method, for solving boundary value problems (BVPs) for linear and integrable nonlinear partial differential equations (PDEs) has received a lot of attention. For linear elliptic PDEs, this method yields two equations, known as the global relations, coupling the Dirichlet and Neumann boundary values. These equations can be used in a collocation method to determine the Dirichlet to Neumann map. This involves expanding the unknown functions in terms of a suitable basis, and choosing a set of collocation points at which to evaluate the global relations. Here, using these methods for the Helmholtz and modified Helmholtz equations and following the earlier results of [15], we determine eigenvalues of the Laplacian in a convex polygon. Eigenvalues are characterised by the points where the generalised Dirichlet to Neumann map becomes singular. We find that the method yields spectral convergence for eigenfunctions smooth on the boundary and for non-smooth boundary values, the rate of convergence is determined by the rate of convergence of expansions in the chosen Legendre basis. Extensions to the case of oblique derivative boundary conditions and constant coefficient elliptic PDEs are also discussed and demonstrated.

© 2017 IMACS. Published by Elsevier B.V. All rights reserved.

1. Introduction

In the late nineties, a new method for analysing boundary-value problems (BVP) for linear and for integrable nonlinear partial differential equations (PDEs) was introduced by the second author [16–18]. This method, which has become known as the unified transform or the Fokas method, has been applied to a variety of linear elliptic PDEs formulated in the interior (and exterior) of a polygon. One can think of the method as a generalised Fourier transform, each transform being tailored to the PDE at hand. For the Laplace, modified Helmholtz and Helmholtz equations, the method expresses the solution in terms of integrals in the complex Fourier plane. However, these integrals contain integral transforms of both the Dirichlet and Neumann boundary values. These representations are analogous to the classical Green's representations, but they are formulated in the Fourier space as opposed to physical space. The transforms of the Dirichlet and Neumann boundary values are coupled via two algebraic equations – the global relations. This method has been used to obtain solutions where classical methods fail [21,43] and has been put on a rigorous footing by Ashton [1,2].

* Corresponding author.

E-mail addresses: mjc249@cam.ac.uk (M.J. Colbrook), tf227@cam.ac.uk (A.S. Fokas).

There has been considerable interest in using the global relations to evaluate numerically the generalised Dirichlet to Neumann map [20,22,15,23,37–40,42,27]. The general approach can be summed up in two steps. First, one expands the unknown boundary values in some suitable basis. The choice of the basis can significantly improve the convergence properties of the method. We will chose Legendre polynomials since their Fourier transform can be expressed via modified Bessel functions and they have been demonstrated to have good convergence properties for the method. Next, one evaluates the approximate global relation using these expansions at suitable collocation points. This gives a finite linear system of equations which, assuming the generalised Dirichlet to Neumann map is not singular, can be inverted for an approximation of the unknown boundary values. It is found that over-determining the system yields smaller condition numbers. Here, we take advantage of recent developments in this area [42,27] in our choice of collocation points. The method can also be adopted to form a Galerkin scheme by integrating the global relations [2,6].

In this paper, we use the above method to study the generalised Dirichlet to Neumann map when it becomes singular. It is shown that the points where the map becomes singular correspond precisely to eigenvalues. A scheme for computing these eigenvalues and eigenfunctions is introduced and its effectiveness is demonstrated on a range of examples with different boundary conditions. We find that the method yields spectral convergence, analogous to the convergence demonstrated for this method when inverting the Dirichlet to Neumann map. The eigenvalue/eigenfunction problem has many applications in engineering and physics [14,8,34] and in data analysis [36]. In two dimensions it is known as the ‘drum’ problem [29,24,31,44]. There are only a handful of domains for which the solution is known analytically and hence a numerical approach is needed. Indeed, there is a vast literature on numerical methods for this problem [10,31]. In general, obtaining eigenvalues of elliptic PDEs with standard methods, such as finite element or finite difference, is problematic, yielding only algebraic convergence and becoming impractical for large eigenvalues. The method presented here yields a diagonally dominant matrix, which is much smaller than standard discretisation methods, and its size in general grows linearly with the number of basis functions used. Furthermore, the method avoids completely the issue of evaluating singular integrals, which appear in boundary-integral equation methods and corresponding boundary-based discretisation methods. An apparent deficiency of the new method is the need to analyse a non linear eigenvalue problem. In practice, this is not an issue since the method is very easily parallelisable. We also find that very small system sizes are needed to obtain high accuracy in spectral data. The idea of using the Fokas method to compute eigenvalues was first presented in [15] in the case of a trapezium. Here, we implement this idea to a variety of examples, compute eigenfunctions and demonstrate that the convergence rate is determined by the convergence rate of the Legendre basis expansion.

The paper is organised as follows: in Section 2 we introduce the global relation and show that non trivial solutions correspond precisely to eigenvalues and eigenfunctions. Section 3 introduces the discretisation method, the choice of collocation points and reviews other methods found in the literature. In Section 4, we demonstrate the method on examples with known spectral data, compare to the finite element method and also demonstrate how eigenvalue multiplicities and eigenspaces can be computed. Section 5 analyses examples with unknown spectrum where we demonstrate convergence rates expected from the asymptotics of corner singularities, whereas Section 6 uses the modified Helmholtz equation to deal with negative eigenvalues. In Section 7, we extend the method to more general constant coefficient elliptic PDEs, and Section 8 discusses further the results presented in this paper.

2. Global relation

Our aim is to solve the eigenvalue problem

$$-u_{xx} - u_{yy} = \lambda u, \quad (x, y) \in \Omega, \quad (1)$$

$$\delta_j u_j^{\mathcal{N}} - \gamma_j u_j = 0 \quad \delta_j = \sqrt{1 - \gamma_j^2}, \quad \gamma_j \in [-1, 1], \quad j = 1, \dots, n, \quad (2)$$

for some bounded convex polygon Ω with sides $\{\Gamma_j\}_{j=1}^n$, where $u_j^{\mathcal{N}}$ denotes the normal derivative along side j . The constants $\{\gamma_j\}$ prescribe Robin boundary conditions along each side, which can be made precise in a trace sense. It is known, that these boundary conditions give rise to a self-adjoint operator, bounded below with compact resolvent whose eigenfunctions form a complete basis of $L^2(\Omega)$ (see [33] Theorem 4.12). The sign of the eigenvalues depends on the sign of γ_j . Dirichlet, Neumann or negative γ_j give rise to non-negative eigenvalues (formally justified by integration by parts). We shall be predominantly interested in this case, but we will demonstrate that our method also works for negative eigenvalues by using the modified Helmholtz equation. For non-negative eigenvalues we may write $\lambda = k^2$ and recast the eigenvalue problem as a non-zero solution to the Helmholtz equation

$$u_{xx} + u_{yy} + k^2 u = 0, \quad (x, y) \in \Omega, \quad (3)$$

$$\delta_j u_j^{\mathcal{N}} - \gamma_j u_j = 0, \quad j = 1, \dots, n. \quad (4)$$

We briefly recall the unified transform method used to solve the Helmholtz equation [20,5]. Letting $z = x + iy$ and $\bar{z} = x - iy$ we have that $V = \exp\left((-ik/2)[\lambda z + \bar{z}/\lambda]\right)$ is a solution of the Helmholtz equation for all $\lambda \in \mathbb{C} \setminus \{0\}$. This allows us to write the PDE in divergence form,

$$\left[V \left(\frac{\partial u}{\partial z} + i \frac{ku\lambda}{2} \right) \right]_{\bar{z}} - \left[V \left(\frac{\partial u}{\partial \bar{z}} + i \frac{ku}{2\lambda} \right) \right]_z = 0. \tag{5}$$

Then, Green’s theorem and simple algebraic manipulation yield the global relation

$$\oint_{\partial\Omega} \exp \left((-k/2)[\lambda z + \bar{z}/\lambda] \right) \left(u^{\mathcal{N}} ds + \frac{ku}{2} (\lambda dz - \frac{1}{\lambda} d\bar{z}) \right) = 0, \quad \lambda \in \mathbb{C} \setminus \{0\}. \tag{6}$$

If u is real then we obtain a second global relation via Schwartz conjugation (i.e. via taking the complex conjugate and then replacing $\bar{\lambda}$ with λ). In our case we can assume without loss of generality that our eigenfunctions are real valued and will do so unless otherwise stated.

For the case of a convex polygon, we denote the corners in anticlockwise order as $\{z_j\}_1^n$. We can parametrise the side Γ_j , joining z_j to z_{j+1} (with the convention that $z_{n+1} = z_1$) by

$$z = m_j + th_j, \quad t \in [-1, 1], \tag{7}$$

with $m_j = (z_j + z_{j+1})/2$ the midpoint and $h_j = (z_{j+1} - z_j)/2$ the relevant direction. Noting that $ds = |h| dt$, this means that we can write the global relation as

$$\sum_{j=1}^n \exp \left((-ik/2)[\bar{m}_j/\lambda + \lambda m_j] \right) \int_{-1}^1 \exp \left((-ikt/2)[\bar{h}_j/\lambda + \lambda h_j] \right) \left(u_j^{\mathcal{N}} |h_j| + \frac{ku_j}{2} (\lambda h_j - \frac{\bar{h}_j}{\lambda}) \right) dt = 0. \tag{8}$$

If we write the unknown boundary values as $v_j = \gamma_j u_j^{\mathcal{N}} + \delta_j u_j$ along each side Γ_j then (8) becomes

$$\sum_{j=1}^n \exp \left((-ik/2)[\bar{m}_j/\lambda + \lambda m_j] \right) \int_{-1}^1 \exp \left((-ikt/2)[\bar{h}_j/\lambda + \lambda h_j] \right) v_j \left(\gamma_j |h_j| + \delta_j \frac{k}{2} (\lambda h_j - \frac{\bar{h}_j}{\lambda}) \right) dt = 0. \tag{9}$$

Our aim will be to estimate k such that the above is satisfied for a non-zero $v \in L^2(\partial\Omega)$. Suppose k^2 is not an eigenvalue and that $v \in L^2(\partial\Omega)$ satisfies (9), then it can be shown that such a v corresponds to the relevant boundary data of a solution of the Helmholtz equation with the homogenous Robin conditions (see [1] and the generalisations therein). But then such a v must be zero otherwise we would have an eigenfunction. Conversely, suppose that k^2 is an eigenvalue with eigenfunction u . It can be shown that for the boundary problem considered here on a convex polygon, u and its normal derivatives¹ lie in $L^2(\partial\Omega)$ [48]. Furthermore, Green’s theorem holds [26] and v must be a non-zero function which satisfies (9). Hence we are essentially looking for k such that the generalised Dirichlet to Neumann map

$$\delta_j u_j^{\mathcal{N}} - \gamma_j u_j \leftrightarrow \gamma_j u_j^{\mathcal{N}} + \delta_j u_j, \quad j = 1, \dots, n, \tag{10}$$

becomes singular by estimating a pair (v, k) that satisfy (9) with non-zero $v \in L^2(\partial\Omega)$. Our strategy is to form an appropriate discretisation of (9) and of the second global relation, and to use these equations in order to construct approximate eigenvalues and eigenfunctions. Eigenvalues of multiplicity greater than one will also be discussed.

Remark 1. In the case of the Dirichlet problem, it can be shown that an eigenfunction actually lies in $H^2(\Omega)$ (see [26] Theorem 3.2.1.2) and hence the trace theorem for curvilinear polygons (see [26] Theorem 1.5.2.1) implies that $u_j^{\mathcal{N}} \in H^{1/2}(\Gamma_j)$ for $j = 1, \dots, n$. In fact, the smoothness depends crucially on the angle of the corners of the polygon. In any neighbourhood where $\partial\Omega$ is analytic, the eigenfunction can be analytically continued across the boundary [44,31]. By multiple reflections, it can also be continued across any corner of angle π/m with $m \in \mathbb{Z}$. For general angle π/α , the singularity at the corner is described in polar coordinates between $\theta = 0$ and $\theta = \pi/\alpha$ by the expression

$$u = Cr^\alpha \sin(\alpha\theta) + o(r^\alpha).$$

We refer the reader to [32] for this result and also to [13] for an explicit form of the singularities. Incorporating these as basis functions in our method is currently under investigation. In Section 5 we shall comment on the expected convergence rate of our method in light of these smoothness results.

In the case that all $\delta_j > 0$, we can use the trace theorem to show that $u_j \in H^{1/2}(\Gamma_j)$ and hence $u_j^{\mathcal{N}} \in H^{1/2}(\Gamma_j)$ for $j = 1, \dots, n$. In particular, these cases include the Neumann and Dirichlet as well as most boundary problems of interest. In general, there exists some $\epsilon_0 > 0$, depending on Ω and the boundary conditions, such that for $0 < \epsilon < \epsilon_0$, $u_j \in H^{3/2+\epsilon}(\Gamma_j)$ and $u_j^{\mathcal{N}} \in H^\epsilon(\Gamma_j)$. This is the best possible estimate [25] and it depends crucially on the convexity of the polygon.

¹ The normal derivative is defined almost everywhere, being undefined at the corners.

3. Approximate global relation and the numerical method

3.1. The method

The typical approach using the uniform transform to evaluate the Dirichlet to Neumann maps for the Laplace, Helmholtz and modified Helmholtz equations, involves the expansion of the unknown boundary values in some basis. If we truncate this expansion, and then evaluate the global relations at appropriate points in the complex plane, we obtain a finite linear algebra problem. Various choices of basis and collocation points can be found in [23,38,20,42,22,37,27]. It appears that the best choice of basis is Legendre polynomials. Indeed, using a Fourier or sine basis can give a linear system in block diagonal form, but these bases only give quadratic convergence for the evaluation of the Dirichlet to Neumann map. If the unknown boundary data are sufficiently smooth, then Chebyshev or Legendre polynomial expansions give faster than algebraic convergence. Furthermore, Legendre polynomials appear to give spectral convergence even in the case of irregular polygons, they give rise to closed form expressions for the relevant integrals and maintain small condition numbers for the algebraic system. Note that the finite bases of Chebyshev or Legendre polynomial expansions are the same, but the conditioning can vary.

We first expand the unknown boundary values in the Legendre polynomial basis on each side and truncate:

$$v_j(t) \approx \sum_{l=0}^{N-1} a_l^j P_l(t), \quad (11)$$

where P_m denotes the m th Legendre polynomial (normalised so that $P_m(1) = 1$). We then let

$$\hat{P}_l(\lambda) = \int_{-1}^1 \exp(-i\lambda t) P_l(t) dt, \quad (12)$$

denote the Fourier transform of P_l . This can be written down explicitly in terms of modified Bessel functions as

$$\hat{P}_l(i\alpha) = \frac{\sqrt{2\pi\alpha}}{\alpha} I_{l+1/2}(\alpha). \quad (13)$$

We then obtain the approximate global relation

$$\sum_{j=1}^n \sum_{l=0}^{N-1} \exp\left((-ik/2)[\bar{m}_j/\lambda + \lambda m_j]\right) \left(\gamma_j |h_j| + \delta_j \frac{k}{2} (\lambda h_j - \frac{\bar{h}_j}{\lambda})\right) \hat{P}_l\left(\frac{k}{2} [\bar{h}_j/\lambda + \lambda h_j]\right) a_l^j = 0. \quad (14)$$

Evaluating at different λ , this can be written in matrix form as

$$A(k)\mathbf{x} = 0, \quad (15)$$

where \mathbf{x} denotes the coefficients of unknown boundary values. Our strategy will be to choose these collocation points such that away from eigenvalues the condition number of $A(k)$ is small, but this condition number blows up as we approach an eigenvalue. We can then extract an approximation to an element in the eigenspace by computing the left singular vector corresponding to the smallest singular value of $A(k)$ and expanding with the corresponding coefficients. After we have computed the unknown boundary values, then we can use either the representation in the uniform transform method [19,43] or the Green's function representation to generate the solution at any interior point of Ω . In the former case, the contours of integration can be deformed to gain rapid convergence.

It is appropriate at this point to mention some standard approximation results about Legendre polynomials since these will play a role in our numerical examples. For $s \geq 0$, let $H^s((-1, 1))$ denote the Sobolev space defined in the usual way for $s \in \mathbb{Z}$ (derivatives of order up to s lie in $L^2((-1, 1))$) and defined by complex interpolation for non integer s (see [9]). Let P_N denote the orthogonal projection onto the first N Legendre polynomials. It was shown in [11] that for any $s \geq 0$, there exists a constant C such that

$$\|f - P_N f\|_2 \leq CN^{-s} \|f\|_{H^s}, \quad \forall f \in H^s((-1, 1)). \quad (16)$$

Similar bounds for the uniform norm can be found in [47], along with a proof that the error (in the uniform or L^2 norm) decays exponentially fast if f can be extended to an analytic function on a neighbourhood of $I = (-1, 1)$ in the complex plane. We will see that this exponential convergence is captured by our method, for smooth enough unknown boundary values v . However, in Section 5 we explore the case when v is singular and for this we will need a refinement of (16).

3.2. Choice of collocation points

Various choices of λ for evaluating the global relation(s) have been proposed in the literature, including Halton nodes [22] or certain rays in the complex plane [27]. Careful choice in the Fourier basis gives a block diagonal system, but this cannot be achieved for our choice of basis. Given a side j , we wish to choose λ such that the terms corresponding to this side are dominant in (14). It was shown in [20] (a similar argument holds for the Helmholtz equation) that for a convex polygon this can be achieved by choosing

$$\frac{k}{2} [\bar{h}_j/\lambda + \lambda h_j] = -\ell \quad (17)$$

for some positive real ℓ . After evaluating the system at this point, and multiplying the resulting system by $e^{ik/2[\bar{m}_j/\lambda + \lambda m_j]}$, we find that the exponential contributions from adjacent sides decay linearly for large ℓ , whereas the contributions from other sides further from side j decay exponentially as $l \rightarrow \infty$. We also want our system to have similar condition numbers as we vary k , hence we choose to evaluate the global relation at the points

$$\lambda = -\frac{2\ell/k + \sqrt{(2\ell/k)^2 - 4|h_j|^2}}{2h_j}. \quad (18)$$

This is done for each side $j = 1, \dots, n$ and ℓ on M evenly spaced points in the interval $[R_1, R_2]$, evaluating the real and imaginary parts to form a matrix $A(k) \in \mathbb{R}^{2nM \times nN}$. This corresponds to evaluating the second global relation at points $\bar{\lambda}$. We take $2M > N$ to ensure the system is overdetermined. For a given choice of N, R_1, R_2 we have found that there exists a threshold above which condition numbers are not reduced by increasing M . We also note that condition numbers depend on R_1, R_2 but we have not attempted to determine the best possible values of R_1, R_2 . The majority of choices produces qualitatively similar results.

In the cited references, the above method used for the evaluation of the generalised Dirichlet to Neumann map (for non homogeneous boundary conditions) away from the eigenvalues of the Laplacian, appears to yield spectral convergence. In other words, the error decreases as $\mathcal{O}(e^{-cN})$ for some constant $c > 0$. Clearly, we cannot hope for such convergence when the boundary data of the eigenfunctions are not smooth on each side with bounded derivatives, however we will demonstrate that for smooth enough data we can also obtain spectral convergence in estimating eigenvalues and eigenfunctions. Furthermore, for the cases of known solutions we find that the error decays like the error in truncating the Legendre expansions of the data. This suggests that other basis choices may be appropriate to incorporate corner singularities. This has been pursued in [22] for the inversion of the Dirichlet to Neumann map but is beyond the scope of this paper.

3.3. Remarks on other methods

There are other methods used to compute eigenvalues/eigenfunctions. The classical boundary integral formulation is based on the Green's function representation of the solution in Ω (understood as a principal value integral on the boundary). Typically, an expansion in terms of Legendre polynomials along the same line will yield spectral convergence (see [35] for a survey of the method and [22] for comparisons with the unified transform for solving Laplace's equation). However, this method suffers from the drawback of the need to evaluate singular integrals. This is possible in closed form for the solution of Laplace's equation [22] but in general can be very difficult. For our problem, the Green's function can be written in terms of a Hankel function and hence the singularity is only logarithmic. Quadrature rules for evaluating such integrals have been proposed [41,30] but can be hard to implement with known error estimates and have been studied extensively in numerical analysis [12]. Hence, it is common to discretise the boundary into a large number of boundary elements which generally leads to only algebraic convergence [45].

Another common method is the finite element method, which yields algebraic convergence rates for the eigenvalues and eigenfunctions (depending on their smoothness) [10]. This method becomes unpractical for large k . Essentially one expects that the mesh width needs to be on order $1/k$ to resolve the eigenfunctions leading to huge system sizes and accuracy is rapidly lost. We shall use this method for comparison with our method for the case of small eigenvalues for polygons where the spectrum is not known analytically.

Finally, we note that a similar idea to our method has been proposed for the Dirichlet problem in [6]. The method in [6] differs in that the global relation is integrated along rays in the complex plane, rather than a collocation method. This allows one to use a Galerkin scheme and it was proven that this gives convergence to the eigenvalues and eigenspaces. However, the condition numbers of the systems grows with k and no numerical convergence analysis is performed in [6] for the eigenvalue problem. Also, each entry of the corresponding matrix must be computed by an integral which can take considerable computing time, (however, in contrast to the integrals appearing in boundary integral methods, the above integrals can be deformed in the complex plane yielding rapid convergence).

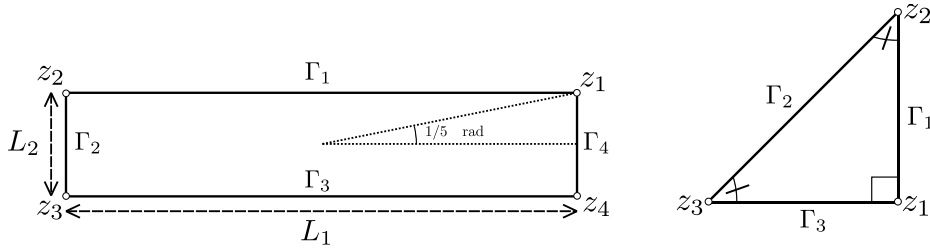


Fig. 1. The rectangle and triangle used for testing the new method. In both cases we can compare explicitly known eigenvalues and eigenfunctions with the numerical results obtained by the new method. The labeling shown will be consistent with later figures.

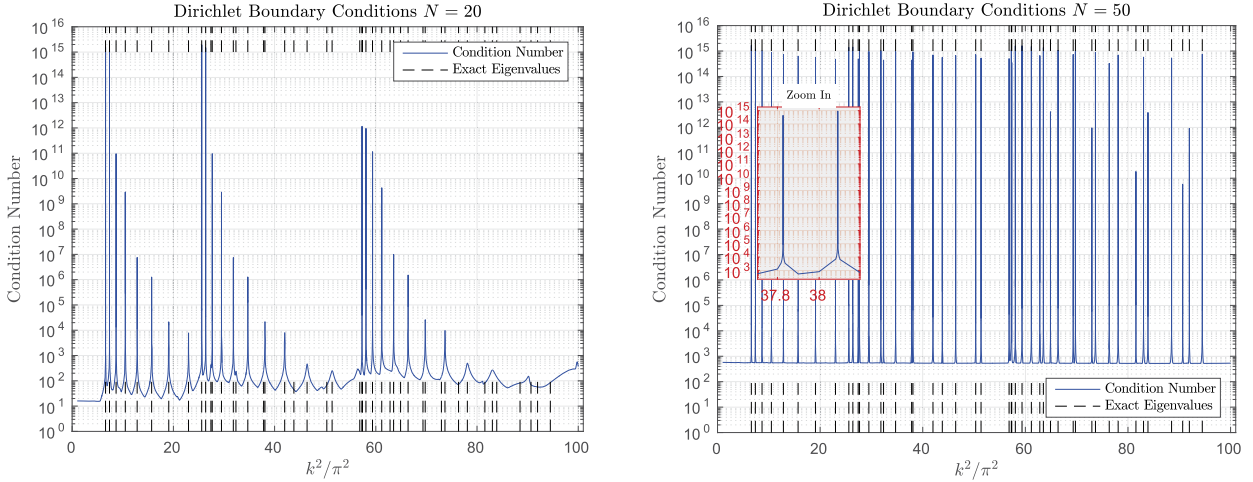


Fig. 2. Left: Condition number plotted against k^2/π^2 for $N = 20$. The analytic eigenvalues are shown as the vertical dashed lines. Right: The same, but for $N = 50$. Note that increasing N helps capture the eigenvalues corresponding to larger wavenumbers.

4. Numerical results for examples with analytic spectrum

In this section we will investigate numerically the proposed method of finding eigenvalues/eigenfunctions for two analytically solvable examples – the rectangle and isosceles right angled triangle. These examples are shown in Fig. 1, where we use scalings so that all vertices lie on the unit circle. We have also tested the method on parallelograms, on the equilateral triangle and on a triangle with angles $\pi/2, \pi/3, \pi/6$ and have obtained similar results.

4.1. Rectangle

We begin with the Dirichlet problem corresponding to $\gamma_j = 1$. Following [27] we choose $M = 2nN$ and set $R_1 = 1, R_2 = 5N/2$. If one is only interested in a small interval of eigenvalues, then different choices may be more suitable, but we have made the above choices in order to study all eigenvalues simultaneously up to $k^2/\pi^2 = 100$. The eigenfunctions/eigenvalues are given by the expressions

$$\sin\left(\frac{m\pi}{L_1}(x - L_1/2)\right) \sin\left(\frac{n\pi}{L_2}(y - L_2/2)\right), \quad \lambda_{m,n} = \pi^2\left(\frac{m^2}{L_1^2} + \frac{n^2}{L_2^2}\right), \quad m, n \in \mathbb{N}. \tag{19}$$

L_1^2 and L_2^2 are incommensurable hence all the eigenvalues are simple. The condition number of the linear system as a function of k is shown in Fig. 2 for $N = 20$ and $N = 50$. We have found that small values of N are sufficient to achieve spikes in the condition number for small wavenumbers. The eigenvalues that have not spiked for $N = 20$ correspond to large m or n , which, due to the two lengths L_1, L_2 , may not physically be the largest eigenvalues. This is expected due to the increasingly oscillatory nature of the Neumann boundary conditions as $\lambda_{m,n}$ increases.

Fig. 2 suggests the following strategy for finding eigenvalues. A local search routine is used to find the maximum of the condition number in the vicinity of a sharp spike. We can also estimate the unknown Neumann boundary value along each side by computing the singular vector corresponding to the smallest singular value. The absolute error of k^2/π^2 and the $L^2(\partial\Omega)$ error of the approximate eigenfunction are shown in Fig. 3 for both large and small eigenvalues. We stress that we chose k according to the eigenvalue estimates – we did not use the analytically known values. We measure the error in the eigenfunctions by first normalising to $\|v\|_{L^2(\partial\Omega)} = 1$ and then computing the quantity

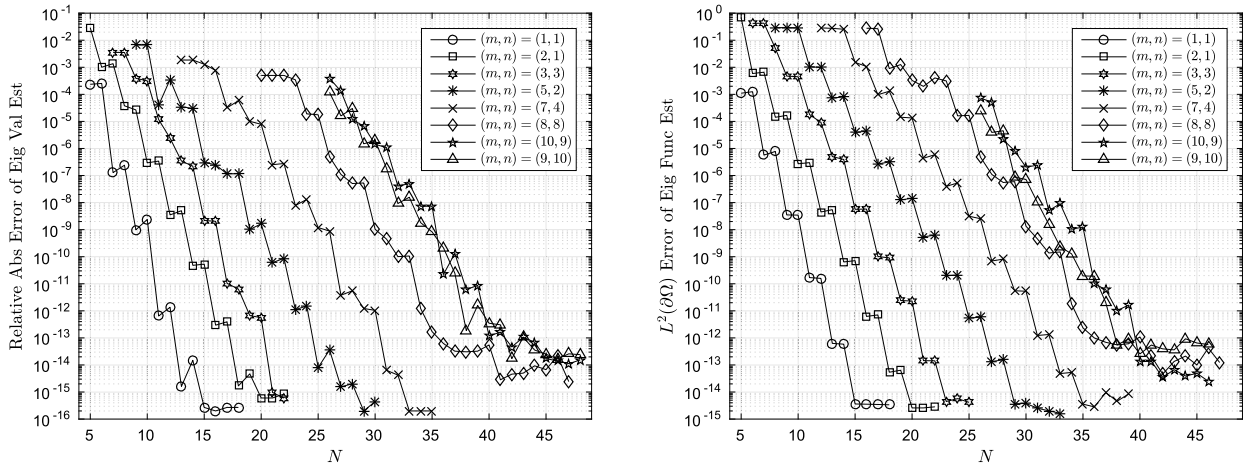


Fig. 3. Left: The error in approximating a representative selection of eigenvalues. Right: The corresponding $L^2(\partial\Omega)$ error in re-constructing the unknown boundary values v .

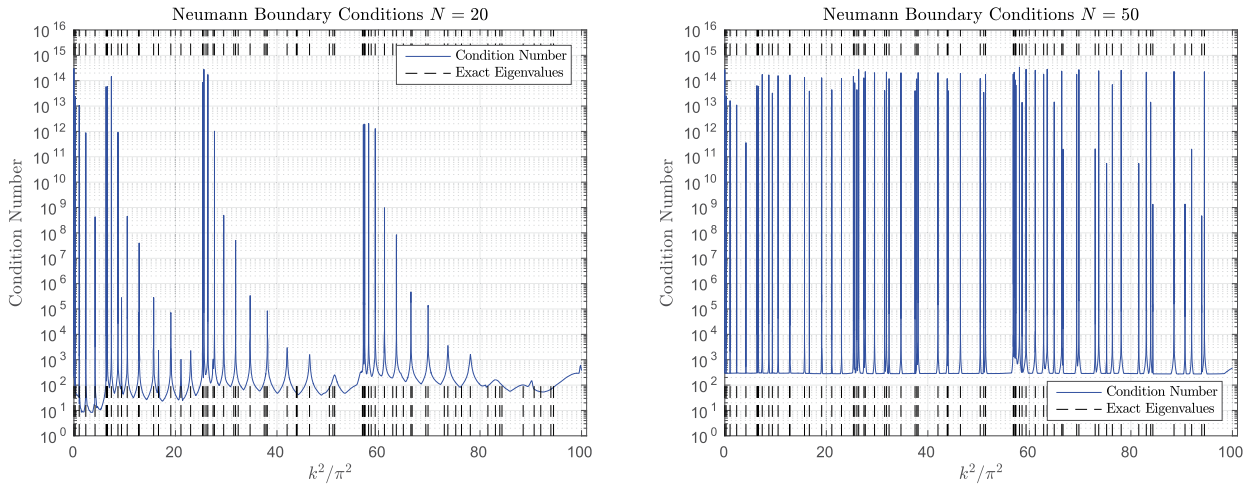


Fig. 4. The same as in Fig. 2 but for the Neumann problem.

$$\inf_{g \in E} \|v - g\|_{L^2(\partial\Omega)}, \tag{20}$$

where E is the corresponding eigenspace. This computation is straightforward once we normalise our Legendre polynomials to an orthonormal basis.

It is clear that the method has spectral convergence. The approximation quickly yields machine precision with a larger minimum error for approximating larger eigenvalues. The slopes corresponding to the L^2 error have exactly the same gradient as the error obtained from truncating the Legendre basis series, indicating that the spectral convergence is inherited from the spectral convergence of Legendre polynomial expansions. The staircase effect can be understood via the parity of the Legendre unctons and Neumann boundary values.

Figs. 4 and 5 depict the corresponding plots for the Neumann boundary conditions. Here the spectral data are

$$\cos\left(\frac{m\pi}{L_1}(x - L_1/2)\right) \cos\left(\frac{n\pi}{L_2}(y - L_2/2)\right), \quad \lambda_{m,n} = \pi^2\left(\frac{m^2}{L_1^2} + \frac{n^2}{L_2^2}\right), \quad m, n \in \mathbb{N}. \tag{21}$$

The same conclusions can be drawn: for larger wavenumbers spectral accuracy is achieved but larger N is needed. Finally, note that an $L^2(\partial\Omega)$ bound on the approximated eigenfunctions can easily be converted to an $L^\infty(\Omega)$ bound using integral representations such as the Green's function representation. Hence, the method can be used to achieve spectral accuracy in the $L^\infty(\Omega)$ norm.

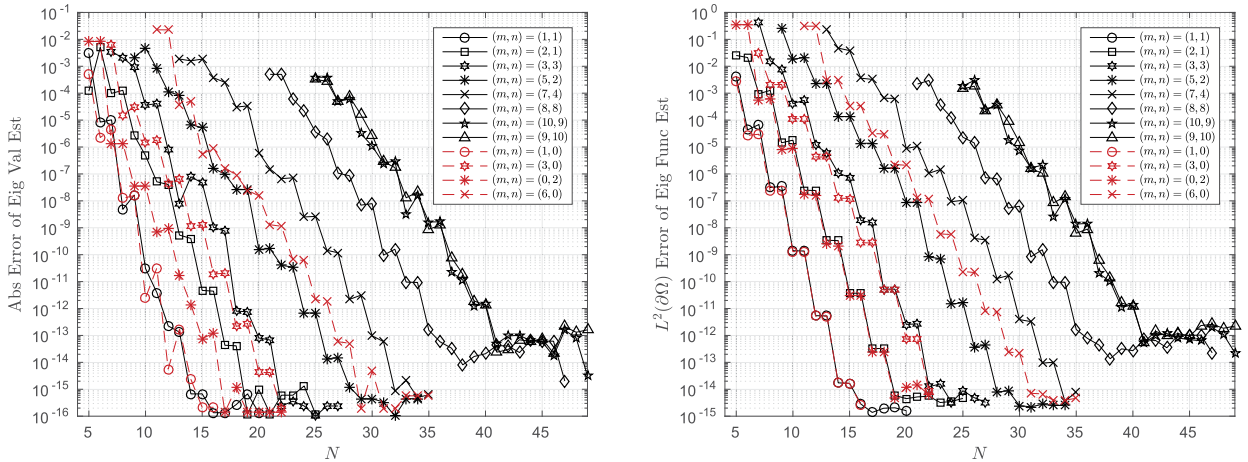


Fig. 5. The same as in Fig. 3 but for the Neumann problem.

4.2. Comparison with FEM

Here we briefly compare the above method to the finite element method (FEM). Other methods such as boundary integral methods without interior discretisations may also be possible (see [22] for an example with the Laplacian) but we stick to FEM for simplicity and since it is arguably the most common method. Fig. 6 shows the relative error in approximating eigenvalues and the $L^2(\Omega)$ error in approximating eigenfunctions against the mesh diameter h for the Dirichlet problem.² We have used quadratic elements and have found that the eigenvalue error decays like $\mathcal{O}(h^4)$ and the eigenfunction error decays like $\mathcal{O}(h^3)$, consistent with [10]. Most standard methods, such as finite difference, finite elements, boundary elements or their relatives, will at best produce algebraic convergence.³ Furthermore, the size of the system in two dimensions grows as $\mathcal{O}(1/h^2)$ (or $\mathcal{O}(1/h)$ for boundary elements), with very small h needed to compute eigenvalues with larger wavenumbers. For our rectangle, a 598199×598199 system was needed for $h = 0.002$, making such methods impractical for large eigenvalues. The sparsity pattern of the matrix is shown in Fig. 6, demonstrating that it is far from banded. The difficulties described above mean that it is very hard to estimate eigenvalues with wavenumbers larger than those shown in the plot.

On the other hand, the system sizes obtained via our method grow linearly with N , with all system sizes considered in this paper at most of order 1000. The apparent disadvantage of the proposed method is its reduction to a non linear eigenvalue problem. This means that one has to adopt a local search routine for eigenvalues/eigenfunctions. However, in practice we have found that this was outweighed by the small system sizes used, particularly for larger eigenvalues and improved rate of convergence compared to FEM. Another advantage of the new method is that it is easily parallelisable – one simply splits up the domain of interest and performs local searches separately. This is particularly useful if one wants to study a selection of very large eigenvalues. One may also adapt the method by changing the number of basis functions in the expansion truncation on each side separately – it is entirely straightforward to have adaptive refinement.

4.3. Isosceles right angled triangle

Next we test the method on a right-angled triangle with vertices at $1, i, -i$. Up to a re-orientation of the triangle, the Dirichlet spectral data can be written in the form

$$\sin\left(\frac{m\pi}{\sqrt{2}}x\right)\sin\left(\frac{n\pi}{\sqrt{2}}y\right) - \sin\left(\frac{n\pi}{\sqrt{2}}x\right)\sin\left(\frac{m\pi}{\sqrt{2}}y\right), \quad \lambda_{m,n} = \frac{\pi^2}{2}(m^2 + n^2), \quad m, n \in \mathbb{N}, 1 \leq m < n. \quad (22)$$

The Neumann spectral data are similar with cosines replacing sines, a change of sign and $m, n \in \mathbb{Z}_{\geq 0}, 1 \leq m \leq n$. For brevity, here we will only consider the Dirichlet problem and postpone the discussion of the Neumann problem until the section on detecting multiplicities. Note that we can also get eigenvalues of multiplicity greater than 1. This is easily seen by finding numbers that factorise as $m^2 + n^2$ in two different ways, for instance $65 = 1^2 + 8^2 = 4^2 + 7^2$. Fig. 7 shows the corresponding global plot of the condition number for $M = 6N, R_2 = 4N, R_1 = 1$. Note that there are no longer two competing length scales for listing the eigenvalues and hence it seems that eigenvalues best approximated for smaller N correspond to small eigenvalues in a monotonic fashion. Fig. 8 shows the error in approximating the eigenvalues and eigenfunctions for some representative (m, n) (avoiding degeneracies). We see the same spectral convergence as before.

² We have found analogous results for the Neumann problem.

³ Notable exceptions are the hp -FEM and hp -BEM methods.

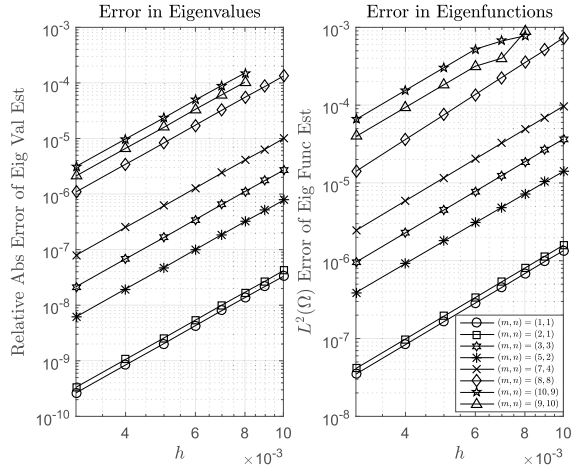
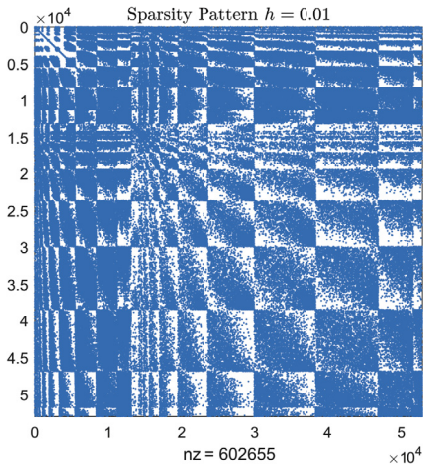


Fig. 6. Left: Sparsity pattern for a typical FEM matrix. Right: The error in approximating eigenvalues and eigenfunctions using the finite elements method. Note that the convergence is algebraic and it requires small h .

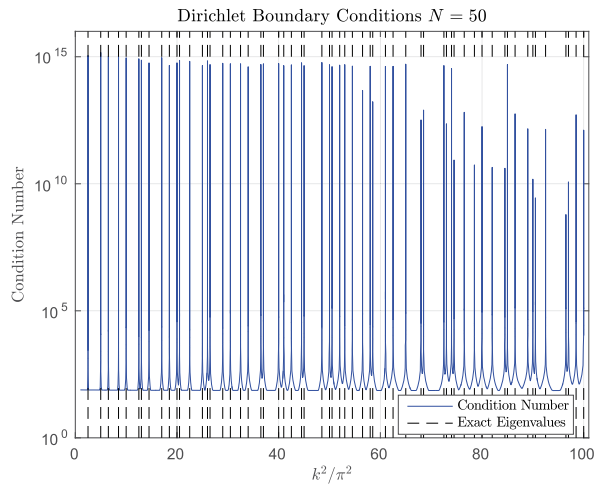
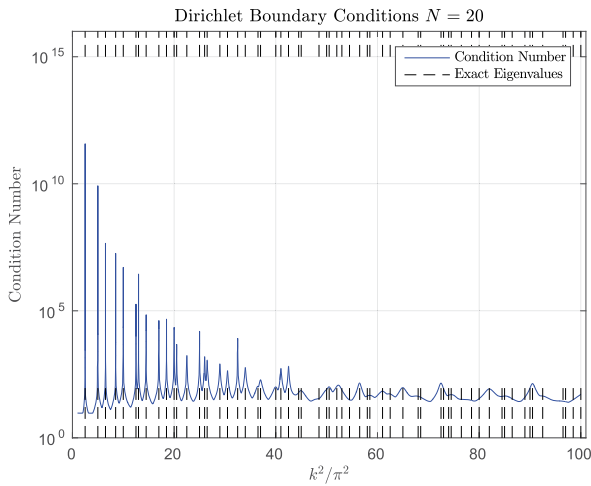


Fig. 7. Condition numbers for $N = 20$ and $N = 50$ for the Dirichlet problem on the triangle. The eigenvalues are well approximated and are monotonic in the parameter N .

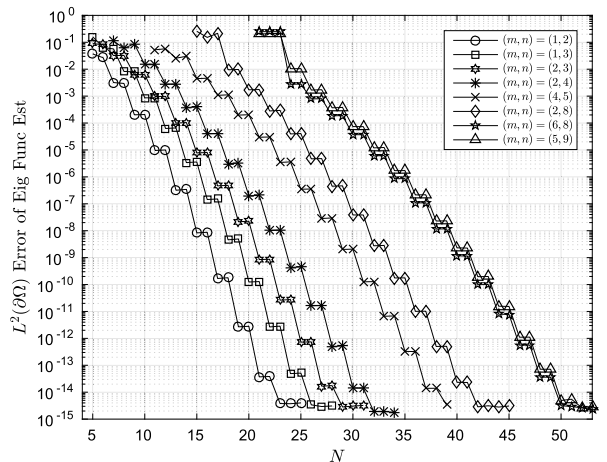
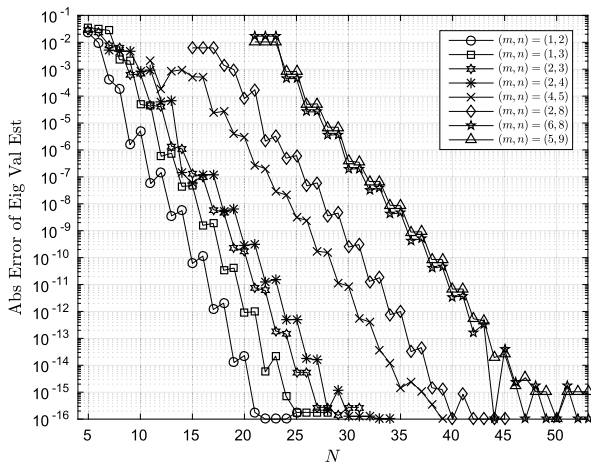


Fig. 8. Left: The error in approximating a representative selection of eigenvalues. Right: The corresponding $L^2(\partial\Omega)$ error in re-constructing the unknown boundary values v . These results are both for the Dirichlet problem on the triangle.

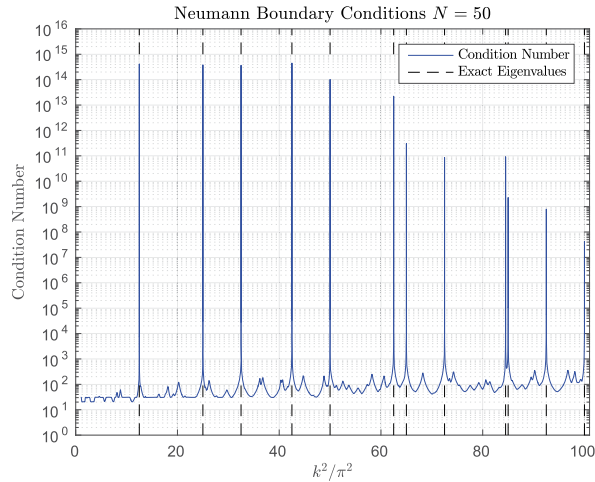


Fig. 9. $\sigma_{nN}(A(k))/\sigma_p(A(k))$ plotted against k^2/π^2 for the Neumann problem on the triangle. The eigenvalues with multiplicity ≥ 2 are shown as vertical dashed lines.

4.4. Multiplicities

In this section we demonstrate that the method can be used to compute eigenvalues of multiplicity greater than one and to approximate the eigenspace. For this we need a distance measure between subspaces. Suppose that $E \subset L^2(\partial\Omega)$ is the eigenspace of unknown boundary values which we approximate via a space $F \subset L^2(\partial\Omega)$. Define

$$\delta(E, F) = \sup_{x \in E, \|x\|=1} \inf_{y \in F} \|x - y\|, \tag{23}$$

and

$$\hat{\delta}(E, F) = \max\{\delta(E, F), \delta(F, E)\}. \tag{24}$$

This notion of distance between subspaces is standard in the literature and is used even in the Banach space case. We will abuse notation and denote the corresponding orthogonal projections of our subspaces by E, F also. In this case we have

$$\delta(E, F) = \sup_{x \in E, \|x\|=1} \inf_{y \in F} \|x - y\| = \sup_{x \in E, \|x\|=1} \|F^\perp x\| = \|F^\perp E\|. \tag{25}$$

We can also write $E - F = F^\perp E - FE^\perp$ as a direct sum with norm $\max\{\|F^\perp E\|, \|FE^\perp\|\}$. Hence it follows that

$$\hat{\delta}(E, F) = \max\{\|F^\perp E\|, \|E^\perp F\|\} = \max\{\|F^\perp E\|, \|FE^\perp\|\} = \|E - F\|. \tag{26}$$

Thus, if we have $E = \text{span}\{u_1, \dots, u_p\}$ with u_j orthonormal (and real WLOG) then the projection can be written in the form

$$E = \sum_{i=1}^p u_i u_i^T. \tag{27}$$

If we expand in terms of a large number of Legendre polynomials, then the above can be approximated very accurately by a finite matrix. To detect eigenspaces of dimension p , we compute the largest singular value of our system A , $\sigma_{nN}(A(k))$, and divide by the p th smallest singular value $\sigma_p(A(k))$. Spikes in the corresponding plot indicate values of k for which k^2 is an eigenvalue of multiplicity p . The collection of left singular vectors v_1, \dots, v_p span our approximation space F . After performing Gram Schmidt, we can easily compute $\hat{\delta}(E, F)$.

Here we only demonstrate results for $p = 2$, but we have tested larger values of p and have found similar results. We test the method on the triangle in Fig. 1 with Neumann boundary data. The eigenvalues/eigenfunctions are

$$\cos\left(\frac{m\pi}{\sqrt{2}}x\right) \cos\left(\frac{n\pi}{\sqrt{2}}y\right) + \cos\left(\frac{n\pi}{\sqrt{2}}x\right) \cos\left(\frac{m\pi}{\sqrt{2}}y\right), \quad \lambda_{m,n} = \frac{\pi^2}{2}(m^2 + n^2), \quad m, n \in \mathbb{Z}_{\geq 0}, 1 \leq m \leq n. \tag{28}$$

The global picture is shown in Fig. 9. We have also shown errors approximations to the eigenvalues and eigenspaces in Fig. 10. It is clear that in this case we also achieve spectral convergence.

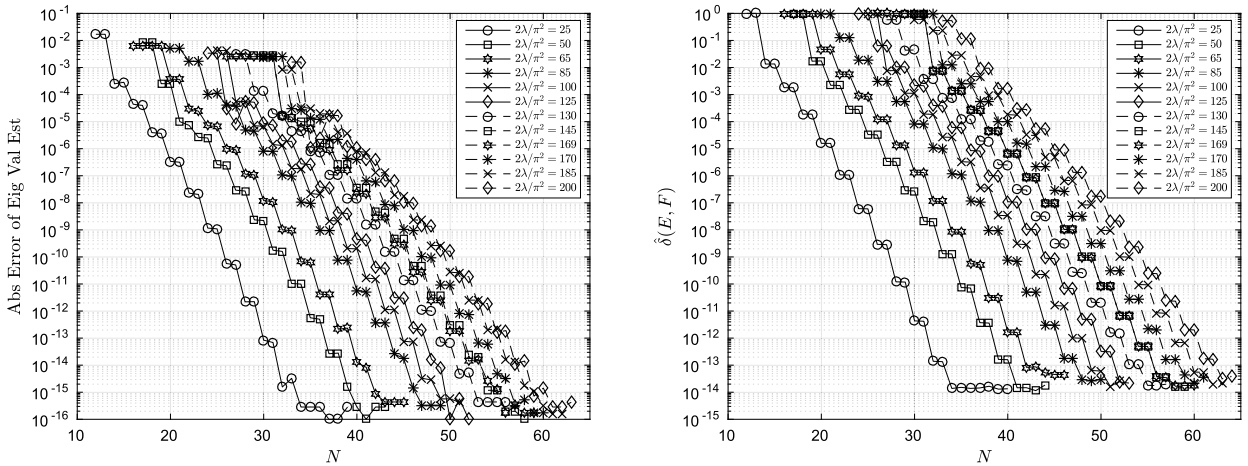


Fig. 10. Left: The error in approximating eigenvalues with a representative selection of eigenvalues. Right: The distance between the approximation eigenspace and the true eigenspace.

5. Numerical results for examples where the spectrum cannot be computed analytically

We now turn to examples where no analytic solutions are known. First, we mention how to take advantage of symmetry (if it is present). If γ_j is independent of j and the polygon is regular, then the collocation matrix has a semi block circulant form

$$A = \begin{bmatrix} A_1 & A_2 & \dots & A_n \\ A_n & A_1 & \dots & A_{n-1} \\ \vdots & \vdots & \ddots & \vdots \\ A_2 & A_3 & \dots & A_1 \end{bmatrix}, \quad A_j \in \mathbb{R}^{2m \times N}. \tag{29}$$

If $M = N$ and the matrix is invertible then its inverse has the following form [46]

$$A^{-1} = \begin{bmatrix} B_1 & B_2 & \dots & B_n \\ B_n & B_1 & \dots & B_{n-1} \\ \vdots & \vdots & \ddots & \vdots \\ B_2 & B_3 & \dots & B_1 \end{bmatrix}, \tag{30}$$

where

$$B_j = \frac{1}{n^2} \sum_{k=1}^n \alpha_k^{j-1} (A^{(k)})^{-1}, \quad \alpha_k = \exp(2\pi(k-1)i/n), \quad A^{(k)} = \frac{1}{n} \sum_{j=1}^n A_j (\bar{\alpha}_k)^{j-1}. \tag{31}$$

This also holds in the least squares sense if $M > N$. In other words, we can look at the maximum condition number of the smaller matrices $\{A^{(k)}\}_{k=1}^n$, which is computationally less expensive. This gives a very fast way of detecting eigenvalues and regions of the parameter k in which to search for eigenvalues. In practice, we found this to be the most time consuming part of our proposed method and hence exploiting symmetry can substantially speed up the relevant procedure.

Suppose also that an eigenspace contains a rotationally symmetric eigenfunction, then we can approximate look at the singularities of the matrix

$$\tilde{A} = \sum_{j=1}^n A_j \in \mathbb{R}^{2M \times N}. \tag{32}$$

Clearly, this will not in general yield approximations to the whole eigenspace (consider multiplicities) and not all eigenvalues are detected, since not every eigenspace contains a non-zero rotationally invariant function.

In this section we shall investigate the regular hexagon and a scalene triangle (whose angles are not rational multiples of π), both with vertices on the unit circle. For the hexagon we consider Dirichlet boundary conditions as well as mixed alternating Dirichlet and Neumann boundary conditions. In the former case we apply the above symmetry considerations. For mixed boundary conditions we can still take advantage of symmetry, but now we need to compute the condition number of 3 (rather than 6) smaller submatrices. For the scalene triangle we consider γ_j chosen uniformly at random. The

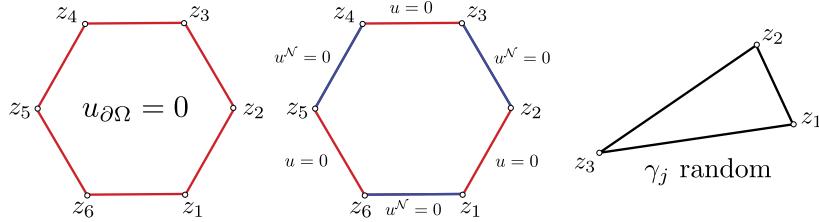


Fig. 11. The domains considered for three examples, for which the spectrum cannot be computed analytically.

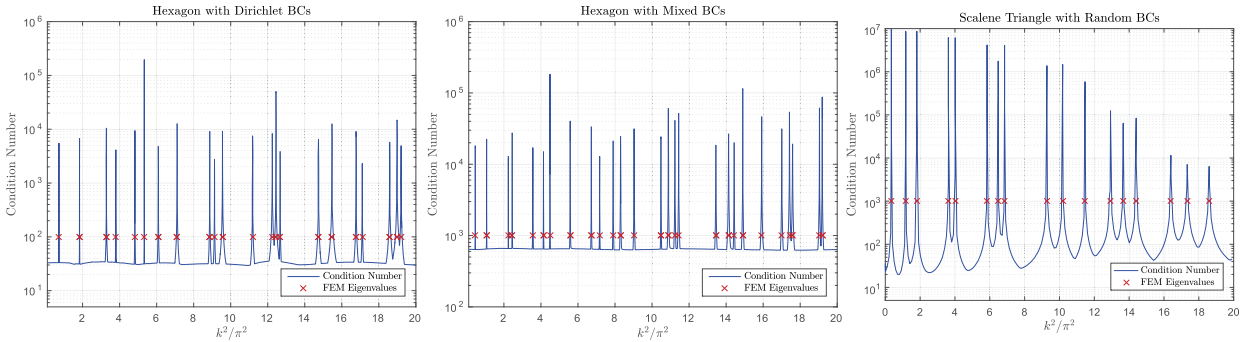


Fig. 12. Condition numbers for $N = 20$ for each domain.

relevant geometries are shown in Fig. 11 and we take $R_1 = 1, R_2 = 2N$ and $M = 8N$. The corresponding condition number plots along with eigenvalues computed via FEM are shown in Fig. 12. Using a smaller spacing in k^2/π^2 causes the spikes to become taller, but we have shown them for a reasonably large k spacing.

The previous examples suggest that for eigenfunctions with smooth enough boundary data, the method yields spectral convergence. However, we do not expect to see spectral convergence in general. Fig. 13 shows the error estimates for eigenvalues (obtained via comparison to large N). We see that algebraic convergence is obtained for some but not all spectral data. In all cases we have found that we can achieve higher precision than FEM by at least a few orders of magnitude for small N . In order to analyse the method, we recall some well known results about the form of corner singularities. Suppose u solves (1), and we consider a corner z_j of Ω . Adopting local polar coordinates such that $z_j = 0$ and $\partial\Omega$ corresponds to $\theta = 0$ and $\theta = \alpha_j$ near the origin, it can be shown (see the references in [13]) that the corner singular functions have the asymptotic form

$$\sum_{p \in \mathbb{Z}_{\geq 0}} \sum_{q=0}^{Q(p)} r^{\lambda+p} \log^q r \phi_{p,q}(\theta), \tag{33}$$

with $\phi_{p,q}(\theta)$ analytic. Here the exponents λ depend on the angle α_j as well as the boundary conditions around z_j . In our case, the leading singularities for the hexagon with Dirichlet boundary conditions, hexagon with Neumann boundary conditions, and scalene triangle with largest angle ω are of the form

$$u_s \sim r^{3/2} \sin(3\theta/2), \quad u_s \sim r^{3/4} \sin(3\theta/4) \text{ and } u_s \sim r^{\pi/\omega} \cos(\theta\pi/\omega), \tag{34}$$

respectively. These can be computed explicitly using the recipe in [13] and are well known in the literature. We now state the following theorem which can be found in [7].

Theorem 1. Let $F(x) = (x + 1)^\gamma \log^\nu(1 + x)$ on $(-1, 1)$ where $\gamma > -1/2$ and $\nu \in \mathbb{Z}_{\geq 0}$. Denoting the orthogonal projection onto the first N Legendre polynomials by P_N , we have for $N \geq \max\{1, \gamma\}$ that

$$\|F - P_N F\|_2 = N^{-(2\gamma+1)} E_\nu(\gamma, N) \left(1 + \mathcal{O}\left(\frac{1}{N}\right)\right), \tag{35}$$

with

$$E_\nu(\gamma, N)^2 = \left(\sum_{k=0}^{\nu} C_{\nu-k}(\gamma) \log^k(1 + N)\right)^2. \tag{36}$$

Furthermore, if γ is not an integer then $C_0 \neq 0$, if γ is an integer and $\nu > 0$ then $C_0 = 0$ but $C_1 \neq 0$. Clearly, if γ is an integer and $\nu = 0$ then there is no approximation error and $E_\nu(\gamma, N) = 0$.

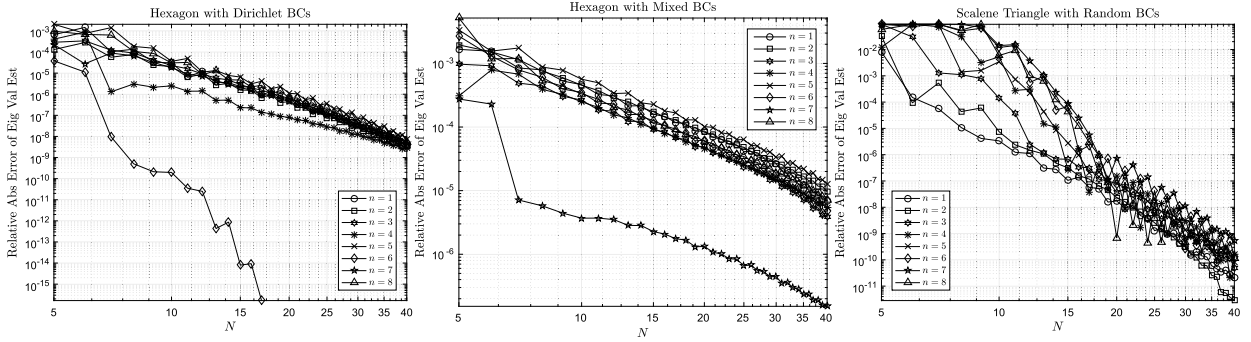


Fig. 13. Error approximates for the first 8 (ignoring multiplicities) eigenvalues for each domain. In the case of the scalene triangle we only considered non-negative eigenvalues (some were negative).

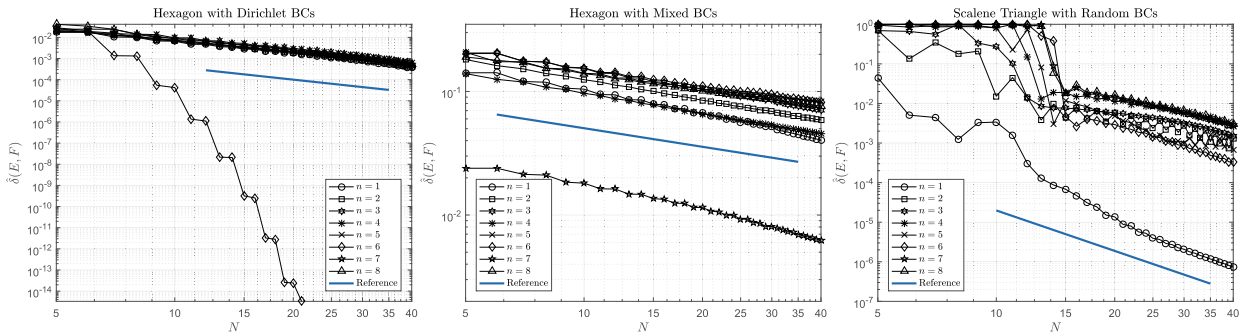


Fig. 14. Error approximates for the first 8 eigenspaces for each domain. We have also shown reference lines displaying the theoretical optimal rate of convergence in the Legendre basis in the presence of the worst singularity.

In the cases considered, there are no logarithmic terms in the leading order and it can be shown that $E_0(\gamma, N) \neq 0$ for non-integer γ . Recalling that we must also compute the normal derivatives for unknown data v , it follows that v for our three problems is approximated via Legendre series with order of convergence 2, 1/2 and ≈ 3.4 respectively. If the worst form of singularities are present, then the above Theorem shows that this is optimal.

The error estimates for eigenfunctions are shown in Fig. 14. In particular, the rate of convergence is similar to that of truncating the Legendre series and we have shown the expected rates of convergence in the presence of corner singularities as reference lines, suggesting faster convergence for smooth eigenfunctions.⁴ Eigenspace number 6 for the hexagon with Dirichlet boundary conditions corresponds to a Dirichlet eigenfunction of an equilateral triangle, rotated six times and then glued together. Hence, the rapid convergence is due to the fact that the Neumann boundary values along each edge can be extended analytically to a neighbourhood of the corresponding edge. The approach of supplementing the Legendre basis with the most singular corner function was demonstrated in [22] for solving Laplace’s equation. Generalising this to Helmholtz type equations is currently under investigation.

6. Negative eigenvalues

In the case of negative eigenvalues, it is necessary to use the modified Helmholtz equation

$$u_{xx} + u_{yy} - k^2 u = 0, \quad (x, y) \in \Omega, \tag{37}$$

$$\delta_j u_j^N - \gamma_j u_j = 0, \quad j = 1, \dots, n. \tag{38}$$

Similar reasoning as earlier [27] leads to the approximate global relation

$$\sum_{j=1}^n \sum_{l=0}^{N-1} \exp\left((ik/2)[\bar{m}_j/\lambda - \lambda m_j]\right) \left(\gamma_j |h_j| + \delta_j \frac{k}{2} \left(\lambda h_j + \frac{\bar{h}_j}{\lambda}\right)\right) \hat{P}_l\left(-\frac{k}{2}[\bar{h}_j/\lambda - \lambda h_j]\right) a_l^j = 0. \tag{39}$$

The choice of collocation points now becomes

⁴ In order to gain this optimal rate of convergence, we found it necessary to increase R_1 to 8 and R_2 to $4N$ in the case of the scalene triangle.

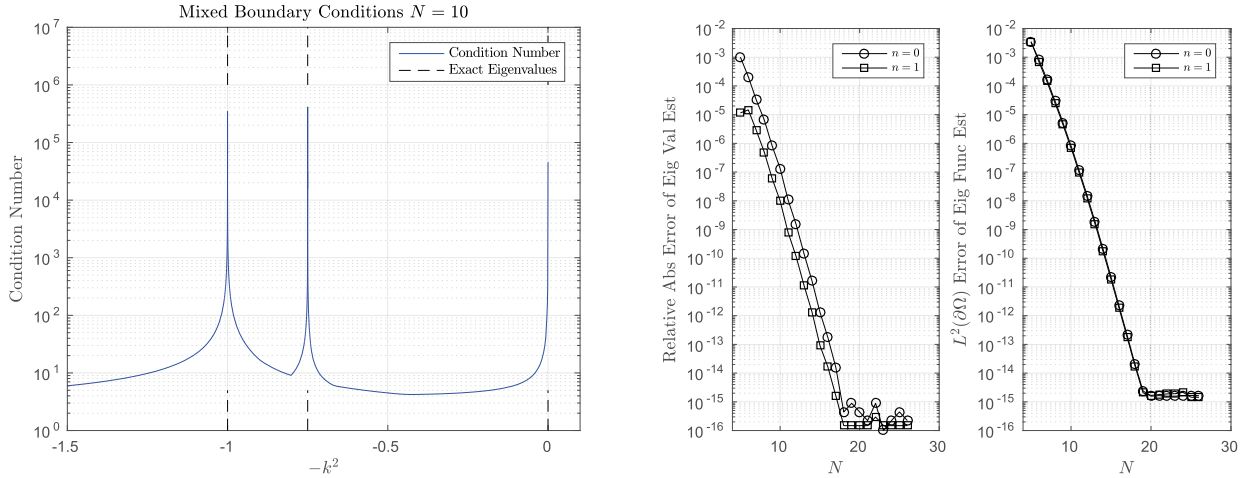


Fig. 15. Left: The condition number for $N = 10$. Right: The errors in eigenvalues and eigenfunctions corresponding to negative eigenvalues. Again we appear to get spectral convergence.

$$\lambda = -\frac{2\ell/k + \sqrt{(2\ell/k)^2 + 4|h_j|^2}}{2h_j}. \tag{40}$$

As before, this is done for each side $j = 1, \dots, n$, with ℓ on M evenly spaced points inside the interval $[R_1, R_2]$, taking the real and imaginary parts of the corresponding relation. In what follows we take $R_1 = 1, R_2 = 5N/2$ and $M = 8N$. For brevity, we only present results for one example, but we have found similar results for other examples. We take the square with side lengths 2π . Neumann boundary conditions are imposed on the top and bottom, whereas $u^N = u$ and $u^N = -u$ are imposed on the right and left sides respectively. The domain is separable and it is straightforward to show that eigenfunctions must be multiples of

$$u(x, y) = \cos\left(\frac{ny}{2}\right)\left(A \exp(\lambda x) + B \exp(-\lambda x)\right), \quad n \in \mathbb{Z}_{\geq 0}, \tag{41}$$

where

$$A(1 - \lambda) \exp(2\pi\lambda) + B(1 + \lambda) \exp(-2\pi\lambda) = 0, \tag{42}$$

$$A(1 - \lambda) + B(1 + \lambda) = 0. \tag{43}$$

For a non trivial solution, $(1 - \lambda^2) \sinh(2\pi\lambda) = 0$. Hence, the collection of negative eigenvalues are -1 and $-3/4$ corresponding to $\lambda^2 = 1$ and $n = 0, 1$ respectively.

Fig. 15 shows the spikes for $N = 10$. We have also demonstrated the spectral convergence to the negative eigenvalues (relative error to k^2) and to the corresponding eigenfunction data $v_j = \gamma_j u_j^N + \delta_j u_j$. Note that there is no stair-casing effect since the boundary values of the eigenfunctions do not have parity on sides 2 and 4.

7. Constant coefficient elliptic PDEs

It is straightforward to employ the method implemented in this paper to the more general eigenvalue problem

$$P(D)u = \lambda u, \quad (x, y) \in \Omega, \tag{44}$$

$$\delta_j u_j^N - \gamma_j u_j = 0 \quad \delta_j = \sqrt{1 - \gamma_j^2}, \quad \gamma_j \in [-1, 1], \quad j = 1, \dots, n, \tag{45}$$

where $D = (-i\partial_x, -i\partial_y)^T$ and $P(D)$ is a second order, constant coefficient elliptic differential operator of the form

$$\sum_{i,j=1}^2 A_{ij} D_i D_j + \sum_{i=1}^2 B_i D_i + C. \tag{46}$$

By a linear change of coordinates (which maps our convex polygon to another convex polygon), we can assume that $A_{ij} = \delta_{ij}$. By setting $q(\mathbf{x}) = \exp(-i\mathbf{B} \cdot \mathbf{x}/2)u(\mathbf{x})$, it is easy to see that $-(\partial_x^2 + \partial_y^2)q = \tilde{\lambda}q$ inside Ω . However, unless we have Dirichlet boundary conditions, we end up with an oblique derivative problem (essentially replacing the Neumann derivative with an oblique derivative). Motivated by the above discussion, we consider mixed Robin and oblique Robin boundary conditions.

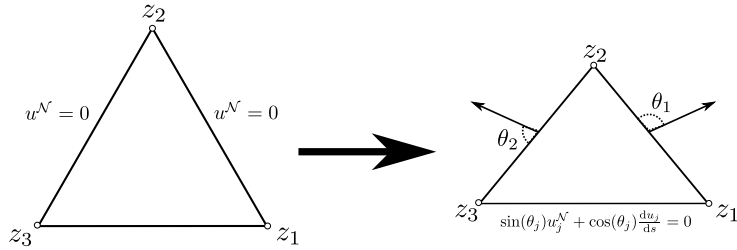


Fig. 16. The domain transformation to an oblique boundary derivative problem.

Suppose we partition the set $S = \{1, \dots, n\}$ into \mathcal{D} and \mathcal{R} such that our boundary conditions become

$$u_j = 0, \quad j \in \mathcal{D}, \tag{47}$$

$$\sin(\theta_j)u_j^N + \cos(\theta_j)\frac{du_j}{ds} - \gamma_j u_j = 0, \quad j \in \mathcal{R}, \tag{48}$$

with $\sin(\theta_j) \neq 0$. This is known as the oblique Robin boundary condition problem and has been studied for the example of an equilateral triangle in [21] and elsewhere [38,37]. Recall that we have the global relation.

$$\oint_{\partial\Omega} \exp\left((-k/2)[\lambda z + \bar{z}/\lambda]\right)\left(u^N + \frac{ku}{2}\left(\lambda\frac{dz}{ds} - \frac{1}{\lambda}\frac{d\bar{z}}{ds}\right)\right)ds = 0, \quad \lambda \in \mathbb{C} \setminus \{0\}. \tag{49}$$

The contributions from the Dirichlet sides were computed earlier; for sides with oblique boundary conditions we substitute u_j^N for $\sec(\theta_j)\gamma_j u_j - \cot(\theta_j)du_j/ds$. Recalling that $ds = |h|dt$ and integrating by parts, the contribution for Γ_j with $j \in \mathcal{R}$ is given by

$$\begin{aligned} \exp\left((-ik/2)[\bar{m}_j/\lambda + \lambda m_j]\right) \int_{-1}^1 e^{(-ikt/2)[\bar{h}_j/\lambda + \lambda h_j]} u_j \left(\frac{\gamma_j |h_j|}{\sin(\theta_j)} + \frac{k}{2}\left(\lambda h_j - \frac{\bar{h}_j}{\lambda}\right) - \cot(\theta_j)\frac{ik}{2}\left(\lambda h_j + \frac{\bar{h}_j}{\lambda}\right)\right) dt \\ - \exp\left((-ik/2)[\bar{m}_j/\lambda + \lambda m_j]\right) \left(\exp\left((-ikt/2)[\bar{h}_j/\lambda + \lambda h_j]\right) \cot(\theta_j)u_j\right)_{t=-1}^{t=+1}. \end{aligned} \tag{50}$$

The formal integration by parts is justified from the remarks on regularity in Section 2. The method of discretisation is exactly as before, but now we have unknown Neumann data on sides $j \in \mathcal{D}$ and unknown Dirichlet data on sides $j \in \mathcal{R}$ with an extra boundary term. Note also that since $u_j \in H^{3/2+\epsilon}(\Gamma_j)$ for some $\epsilon > 0$, we know that the coefficients (with respect to the orthonormal Legendre polynomials) decay like $\mathcal{O}(N^{-3/2-\epsilon})$. The polynomials have magnitude $\mathcal{O}(\sqrt{N})$ and hence it follows that the series converges absolutely uniformly. This means we can include the above boundary terms in our discretisation.

It is possible to write the equation in divergence form and solve along the same lines as Sections 2 and 3. However, we have chosen to adopt this method since it also demonstrates the use of the method for the oblique derivative problem which cannot always be recast as a mixed Robin boundary problem for a constant coefficient elliptic PDE.

For simplicity, we demonstrate the method for an equilateral triangle with vertices $z_1 = 1, z_2 = \sqrt{3}i, z_3 = -1$ and for the operator $2\partial_{yy} + \partial_{xx}$ with Neumann boundary conditions. We change coordinates to $y' = y/\sqrt{2}$ to map to the Laplacian and oblique boundary conditions on sides Γ_1 and Γ_2 with

$$\theta_1 = \arctan\left(\frac{\sqrt{\frac{18}{35}} + \sqrt{\frac{2}{35}}}{\sqrt{\frac{3}{35}} - \sqrt{\frac{12}{35}}}\right) + \pi, \theta_2 = \pi - \theta_1, \theta_3 = \pi/2, \gamma_1 = \gamma_2 = \gamma_3 = 0. \tag{51}$$

This transformation is shown in Fig. 16. In what follows we take $R_1 = 1, R_2 = 6N$ and $M = 6N$. Fig. 17 shows the familiar picture of the condition number (for $N = 50$). We have also shown the eigenvalues calculated using a finite difference eigenvalue solver. The corresponding plot for Dirichlet boundary conditions on the base, is also shown in Fig. 17. For both cases we did observe algebraic instead of spectral convergence and we expect this is due to non-smoothness of the Dirichlet data. Fig. 18 shows a representative plot for the Neumann case where a decay like $\sim \mathcal{O}(N^{-d})$ is observed for $d \approx 6$. Again error in truncating the Legendre series was similar but we noted some eigenfunctions with $d > 7$.

8. Conclusion

We have demonstrated the use of the unified transform (Fokas method) in solving for the spectral data of the Laplacian and general constant coefficient elliptic PDEs in polygonal domains. We provide strong numerical evidence that the

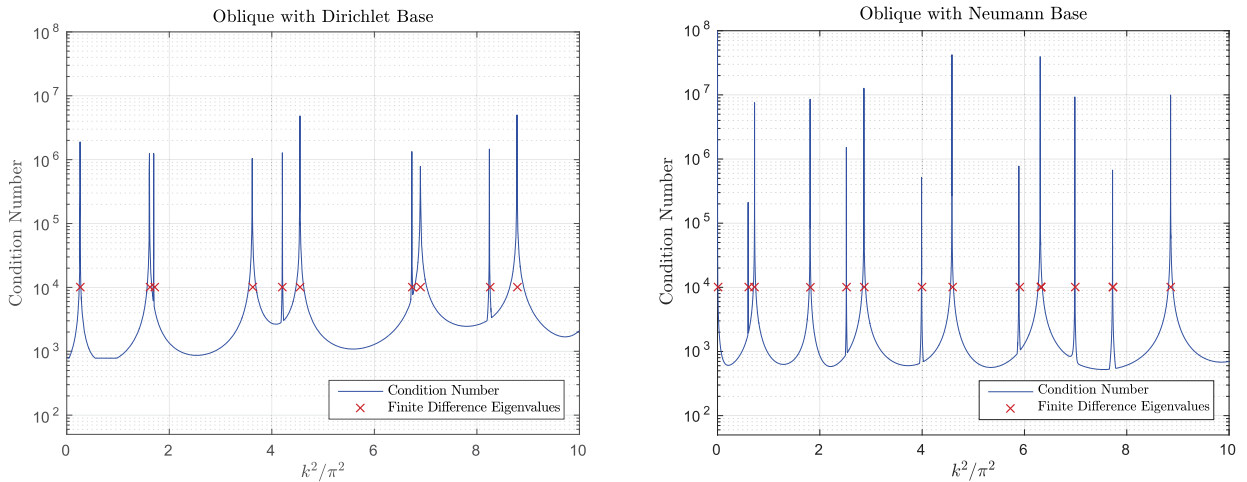


Fig. 17. Left: The condition number plotted against k^2/π^2 for the oblique derivative problem with a Neumann boundary condition on the base, and $N = 50$. Right: Same but with a Dirichlet boundary condition on the base.

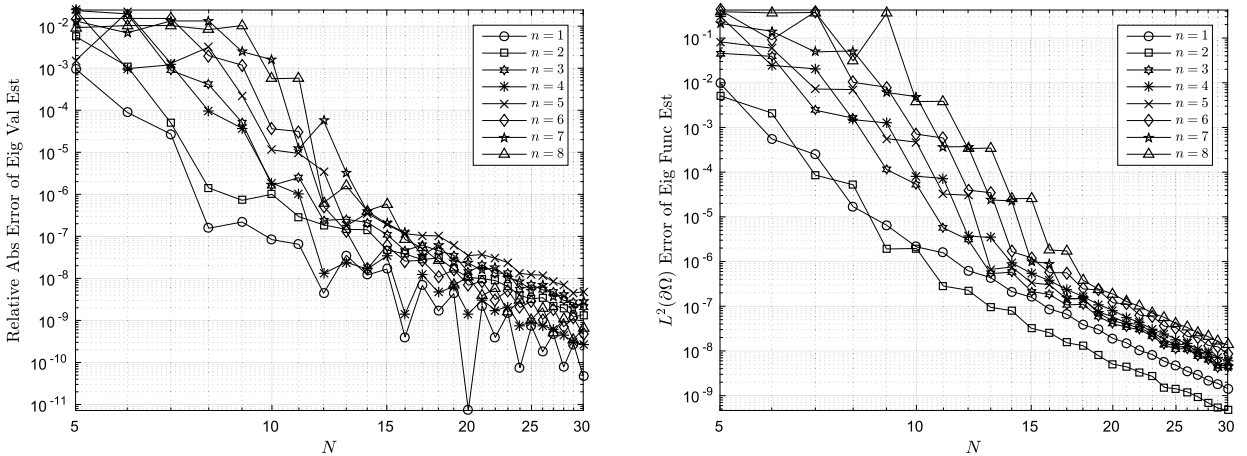


Fig. 18. Errors in the first 8 non-trivial eigenvalues and eigenfunctions for the oblique problem with a Neumann boundary condition on the base. We observed the same curve (slope ≈ -6) for N up to 60.

convergence rate of the method is determined by the regularity of the boundary data of the eigenfunctions, with spectral convergence for smooth enough boundary data. Furthermore, the method is numerically very easy to implement with explicit matrix values listed in Section 3, avoiding both the singular integrals in usual boundary integral methods and the complexity in high order discretisation methods. The method can be easily parallelised and is easily adapted to mixed Robin/Dirichlet/Neumann and oblique derivative boundary problems.

These results fit nicely into recent work on using similar approximations to invert the Dirichlet to Neumann map discussed in the introduction and Section 3. Although no proof of convergence has been provided, there is strong numerical evidence that the method of looking locally for ‘spikes’ in the condition number does converge. We should mention however, that in general the condition number of the system grows with N . The method works since the condition number grows at a much faster rate in the vicinity of an eigenvalue. As mentioned earlier, a similar method involving integrating the global relation has been proven to converge in [6]. The numerical evidence presented here complements the results of [6] and in practice is easier to use, yielding better numerical results with much smaller condition numbers away from eigenvalues at the expense of not having a proof of convergence.

Finally, we discuss extensions. So far the numerical implementations of the unified transform method in the literature have considered planar domains. Recently Ashton has extended the analysis of the Dirichlet to Neumann map to convex polyhedra [3,4]; see also [28]. In future work, these cases will be studied numerically. We have found that the convergence rate of the method follows the convergence rate of the Legendre series of the unknown boundary values. This suggests that other basis choices may be suitable. The inclusion of basis functions with more singular behavior at the corners of the polygon has been mentioned and this will also be the topic of future work.

Acknowledgements

MJC would like to thank Anthony Ashton and Euan Spence for useful discussions on previous collocation methods. MJC acknowledges with gratitude support from EPSRC grant EP/L016516/1 for the University of Cambridge Centre for Doctoral Training, the Cambridge Centre for Analysis. ASF acknowledges with gratitude support from EPSRC in the form of a Senior Fellowship.

References

- [1] A. Ashton, On the rigorous foundations of the Fokas method for linear elliptic partial differential equations, *Proc. R. Soc. A*, vol. 468, The Royal Society, 2012, pp. 1325–1331.
- [2] A. Ashton, The spectral Dirichlet–Neumann map for Laplace's equation in a convex polygon, *SIAM J. Math. Anal.* 45 (6) (2013) 3575–3591.
- [3] A. Ashton, Elliptic PDEs with constant coefficients on convex polyhedra via the unified method, *J. Math. Anal. Appl.* 425 (1) (2015) 160–177.
- [4] A. Ashton, Laplace's Equation on Convex Polyhedra via the Unified Method, *Proc. R. Soc. A*, vol. 471, The Royal Society, 2015.
- [5] A.C. Ashton, et al., The fundamental k-form and global relations, *SIGMA* 4 (033) (2008) 15.
- [6] A. Ashton, K. Crooks, Numerical analysis of Fokas' unified method for linear elliptic PDEs, *Appl. Numer. Math.* 104 (2016) 120–132.
- [7] I. Babuška, B. Guo, et al., Optimal estimates for lower and upper bounds of approximation errors in the p-version of the finite element method in two dimensions, *Numer. Math.* 85 (2) (2000) 219–255.
- [8] I. Babuška, J. Osborn, Eigenvalue problems, *Handb. Numer. Anal.* 2 (1991) 641–787.
- [9] J. Bergh, J. Lofstrom, *Interpolation Spaces: An Introduction*, vol. 223, Springer Science & Business Media, 2012.
- [10] D. Boffi, Finite element approximation of eigenvalue problems, *Acta Numer.* 19 (2010) 1–120.
- [11] C. Canuto, A. Quarteroni, Approximation results for orthogonal polynomials in Sobolev spaces, *Math. Comput.* 38 (157) (1982) 67–86.
- [12] D. Colton, R. Kress, *Integral Equation Methods in Scattering Theory*, SIAM, 2013.
- [13] M. Costabel, M. Dauge, Construction of corner singularities for Agmon–Douglis–Nirenberg elliptic systems, *Math. Nachr.* 162 (1) (1993) 209–237.
- [14] R. Courant, D. Hilbert, *Methods of Mathematical Physics*, vol. 2: Differential Equations, John Wiley & Sons, 2008.
- [15] C.-I.R. Davis, B. Fornberg, A spectrally accurate numerical implementation of the Fokas transform method for Helmholtz-type PDEs, *Complex Var. Elliptic Equ.* 59 (4) (2014) 564–577.
- [16] A.S. Fokas, A unified transform method for solving linear and certain nonlinear PDEs, *Proc. R. Soc. Lond., Ser. A, Math. Phys. Eng. Sci.*, vol. 453, The Royal Society, 1997, pp. 1411–1443.
- [17] A. Fokas, On the integrability of linear and nonlinear partial differential equations, *J. Math. Phys.* 41 (6) (2000) 4188–4237.
- [18] A.S. Fokas, Two-dimensional linear partial differential equations in a convex polygon, *Proc. R. Soc. Lond., Ser. A, Math. Phys. Eng. Sci.*, vol. 457, The Royal Society, 2001, pp. 371–393.
- [19] A.S. Fokas, *A Unified Approach to Boundary Value Problems*, SIAM, 2008.
- [20] A. Fokas, N. Flyer, S. Smitheman, E. Spence, A semi-analytical numerical method for solving evolution and elliptic partial differential equations, *J. Comput. Appl. Math.* 227 (1) (2009) 59–74.
- [21] A. Fokas, K. Kalimeris, Eigenvalues for the Laplace operator in the interior of an equilateral triangle, *Comput. Methods Funct. Theory* 14 (1) (2014) 1–33.
- [22] B. Fornberg, N. Flyer, A Numerical Implementation of Fokas Boundary Integral Approach: Laplace's Equation on a Polygonal Domain, *Proc. R. Soc. Lond., Ser. A, Math. Phys. Eng. Sci.*, vol. 467, The Royal Society, 2011, pp. 2983–3003.
- [23] S. Fulton, A. Fokas, C. Xenophontos, An analytical method for linear elliptic PDEs and its numerical implementation, *J. Comput. Appl. Math.* 167 (2) (2004) 465–483.
- [24] C. Gordon, D. Webb, S. Wolpert, Isospectral plane domains and surfaces via Riemannian orbifolds, *Invent. Math.* 110 (1) (1992) 1–22.
- [25] P. Grisvard, *Singularities in Boundary Value Problems*, vol. 22, Springer, 1992.
- [26] P. Grisvard, *Elliptic Problems in Nonsmooth Domains*, SIAM, 2011.
- [27] P. Hashemzadeh, A. Fokas, S. Smitheman, A Numerical Technique for Linear Elliptic Partial Differential Equations in Polygonal Domains, *Proc. R. Soc. A*, vol. 471, The Royal Society, 2015.
- [28] I. Hitzazis, A. Fokas, Linear elliptic PDEs in a cylindrical domain with a polygonal cross-section, *Stud. Appl. Math.* 139 (2017) 288–321.
- [29] M. Kac, Can one hear the shape of a drum?, *Am. Math. Mon.* 73 (4) (1966) 1–23.
- [30] P. Kolm, V. Rokhlin, Numerical quadratures for singular and hypersingular integrals, *Comput. Math. Appl.* 41 (3–4) (2001) 327–352.
- [31] J. Kuttler, V. Sigillito, Eigenvalues of the Laplacian in two dimensions, *SIAM Rev.* 26 (2) (1984) 163–193.
- [32] R.S. Lehman, Developments at an analytic corner of solutions of elliptic partial differential equations, *J. Math. Mech.* 8 (5) (1959) 727–760.
- [33] W.C.H. McLean, *Strongly Elliptic Systems and Boundary Integral Equations*, Cambridge University Press, 2000.
- [34] K. Nakamura, T. Harayama, *Quantum Chaos and Quantum Dots*, vol. 3, Oxford University Press on Demand, 2004.
- [35] C. Pozrikidis, *A Practical Guide to Boundary Element Methods with the Software Library BEMLIB*, CRC Press, 2002.
- [36] N. Saito, Data analysis and representation on a general domain using eigenfunctions of Laplacian, *Appl. Comput. Harmon. Anal.* 25 (1) (2008) 68–97.
- [37] Y.G. Saridakis, A. Sifalakis, E.P. Papadopoulou, Efficient numerical solution of the generalized Dirichlet–Neumann map for linear elliptic PDEs in regular polygon domains, *J. Comput. Appl. Math.* 236 (9) (2012) 2515–2528.
- [38] A. Sifalakis, A. Fokas, S. Fulton, Y. Saridakis, The generalized Dirichlet–Neumann map for linear elliptic PDEs and its numerical implementation, *J. Comput. Appl. Math.* 219 (1) (2008) 9–34.
- [39] A. Sifalakis, S. Fulton, E. Papadopoulou, Y. Saridakis, Direct and iterative solution of the generalized Dirichlet–Neumann map for elliptic PDEs on square domains, *J. Comput. Appl. Math.* 227 (1) (2009) 171–184.
- [40] A. Sifalakis, E. Papadopoulou, Y. Saridakis, Numerical study of iterative methods for the solution of the Dirichlet–Neumann map for linear elliptic PDEs on regular polygon domains, *Int. J. Appl. Math. Comput. Sci.* 4 (2007) 173–178.
- [41] R. Smith, Direct Gauss quadrature formulae for logarithmic singularities on isoparametric elements, *Eng. Anal. Bound. Elem.* 24 (2) (2000) 161–167.
- [42] S. Smitheman, E.A. Spence, A. Fokas, A spectral collocation method for the Laplace and modified Helmholtz equations in a convex polygon, *IMA J. Numer. Anal.* 30 (4) (2010) 1184–1205.
- [43] E.A. Spence, *Boundary value problems for linear elliptic PDEs*, Ph.D. thesis, University of Cambridge, 2011.
- [44] L.N. Trefethen, T. Betcke, Computed eigenmodes of planar regions, *Contemp. Math.* 412 (2006) 297–314.
- [45] G. Unger, *Analysis of Boundary Element Methods for Laplacian Eigenvalue Problems*, Verlag der Techn. Univ., Graz, 2009.
- [46] R. Vescovo, Inversion of block-circulant matrices and circular array approach, *IEEE Trans. Antennas Propag.* 45 (10) (1997) 1565–1567.
- [47] H. Wang, S. Xiang, On the convergence rates of Legendre approximation, *Math. Comput.* 81 (278) (2012) 861–877.
- [48] N.M. Wigley, Mixed boundary value problems in plane domains with corners, *Math. Z.* 115 (1) (1970) 33–52.